

Growth of $\text{Al}_x\text{Ga}_{1-x}\text{As}/\text{GaAs}$ structures for single quantum wells by solid arsenic MOCVD system

R. Castillo Ojeda, S. Manrique Moreno, M. Galván Arellano and R. Peña-Sierra

CINVESTAV, Instituto Politécnico Nacional,

Depto. de Ing. Eléctrica, SEES.

Apartado postal 14-740, México, D.F. 07000, México

rpsierra@cinvestav.mx; rcastillo-ojeda@yahoo.com.mx

Recibido el 24 de enero de 2007; aceptado el 27 de noviembre de 2007

The results obtained from the growth and characterization of $\text{Al}_x\text{Ga}_{1-x}\text{As}/\text{GaAs}$ multilayer structures by a Metalorganic Chemical Vapor Deposition (MOCVD) system based on metallic arsenic are presented. The MOCVD system was adapted in order to be used for the growth of quantum wells structures. Our main goal is to explore the capability of this growth system for growing high quality multilayer structures, including quantum wells. The use of metallic arsenic to replace the hydride group V precursor (AsH_3), could introduce important differences into the growth process due to the absence of atomic hydrogen. The main electrical and optical characteristics of both GaAs and $\text{Al}_x\text{Ga}_{1-x}\text{As}$ epilayers to be used for the fabrication of multilayer structures are discussed. The assessment of these epilayers and structures was carried out using low temperature photoluminescence (PL), Hall effect measurements, X-ray diffraction, Raman spectroscopy, secondary ion mass spectroscopy (SIMS) and Atomic Force Microscopy (AFM).

Keywords: III-V semiconductors; MOCVD; quantum well structures; electronic properties; optical properties.

Se presentan los resultados del crecimiento y caracterización de estructuras multicapa de $\text{Al}_x\text{Ga}_{1-x}\text{As}/\text{GaAs}$ utilizando un sistema para depositar películas semiconductoras a base de precursores metalorgánicos y arsénico sólido (MOCVD, de Metalorganic Chemical Vapor Deposition). El sistema MOCVD se adaptó para crecer estructuras semiconductoras con pozos cuánticos. El objetivo central de este trabajo fue explorar la capacidad del sistema MOCVD para realizar estructuras de alta calidad, que incluyan pozos cuánticos. El uso de arsénico metálico para sustituir a la arsina como precursor del grupo V (AsH_3), puede introducir diferencias importantes en el proceso de crecimiento por la ausencia de hidrógeno atómico. Se discuten las principales características eléctricas y ópticas de las películas de GaAs y $\text{Al}_x\text{Ga}_{1-x}\text{As}$ usadas en la realización de las estructuras multicapa. La evaluación de las películas y de las estructuras se realizó por mediciones de fotoluminiscencia (PL) a baja temperatura, difracción de rayos-X, espectroscopia Raman, espectroscopia de masas de iones secundarios (SIMS) y microscopia de fuerza atómica (AFM).

Descriptor: Semiconductores III-V; MOCVD; estructuras con pozos cuánticos; propiedades electrónicas; propiedades ópticas.

PACS: 81.05.Ea; 81.15.Gh; 81.07.St; 73.61.Ey; 78.66.Fd

1. Introduction

The Metalorganic Chemical Vapor Deposition (MOCVD) process is now a well developed technique for the growth of III-V semiconductor epitaxial layers [1]. High quality and excellent morphology epilayers are usually achieved. The MOCVD process allows the growth of low dimension multilayer structures with precise control of the thickness, composition and interface quality. However, the technique is not at all free of problems, such as the safety disadvantage for use in large scale device production, because it utilizes considerable quantities of highly toxic gases such as AsH_3 and PH_3 . Those substances are generally handled in high pressure cylinders, thus increasing the danger by potential toxic gas leakages [2].

An attractive solution to this security issue is to find much less hazardous group V sources. Various possibilities, solid arsenic is the least hazardous source, it can be used below the sublimation point, where its vapor pressure is high but controllable. Moreover, solid arsenic is safe due to its low vapor pressure at room temperature, and it is easy to storage [3].

Although solid arsenic is much less hazardous than AsH_3 , the price of by this replacement could be the limited quality

of the materials grown. In this work we report on the production of relative complex semiconductor structures using a MOCVD-solid arsenic based system. The MOCVD system operates at one atmosphere of pressure with a horizontal configuration. We expect that in the future, this alternate MOCVD system can be used for the production of electronic devices. In this work we explore the resulting characteristics of $\text{Al}_x\text{Ga}_{1-x}\text{As}/\text{GaAs}$ multilayer structures grown with this alternate MOCVD system. Initially the electrical and optical characteristics of the $\text{Al}_x\text{Ga}_{1-x}\text{As}$ and GaAs layers were evaluated using low temperature photoluminescence (PL), Hall effect measurements, X-Ray diffraction, Raman spectroscopy, and Atomic Force Microscopy (AFM). Then interfacial properties of the $\text{Al}_x\text{Ga}_{1-x}\text{As}/\text{GaAs}$ structures were analyzed by secondary ion mass spectroscopy (SIMS).

2. Experimental

The growth runs were done on both Si-doped and semi-insulating (100) GaAs substrates, 4° misoriented toward the (110) direction. The substrate preparation involves, as usual, degreasing by organic solvents, surface oxide elimination by HCl and a soft surface chemical etching using

$\text{H}_2\text{SO}_4:\text{H}_2\text{O}_2:\text{H}_2\text{O}$ (5:1:1). In a final step the substrates were thoroughly rinsed in deionized water, and finally the GaAs wafers were dried by nitrogen blowing to eliminate any trace water.

The samples were grown using electronic grade trimethylgallium (TMG) and trimethylaluminum (TMA) as gallium and aluminum precursors, respectively, and metallic arsenic (9N) as the arsenic source. The main characteristics of the MOCVD reactor were reported earlier [4]. The MOCVD system consists of a horizontal quartz tube operating at one atmosphere of pressure. The substrates were located on a graphite substrate holder and heated by infrared lamps. The arsenic supply is controlled by a second independent furnace. The III/V ratio used in the growth runs can be easily adjusted by controlling the arsenic source temperature or by controlling the hydrogen flow through the metalorganic vessels by means of electronic mass flow controllers (MFC). The growth atmosphere consists of palladium purified hydrogen (H_2). The main H_2 flux used was fixed at 8 liters/min.

The PL measurements were carried out using a double SPEX monochromator with a S1 type photomultiplier tube as detector. As a PL exciting source, a He-Ne laser with emission at $\lambda = 632.8$ nm and 20 mW of nominal power was used. Low temperature (12 K) measurements were done with a He closed cycle cryostat. Raman scattering experiments were performed at 300 K using the 5145 Å line of an Ar laser at normal incidence for excitation. Scattered light was analyzed using a Jobin-Yvon T64000 triple spectrometer, operating in the subtractive configuration, and a multichannel charge-coupled device detector cooled at 140 K using liquid nitrogen. The epilayers were measured by HRXRD, using a Bartels monochromator in the Ge (022) reflection mode, with a Cu anode as the source of X-ray radiation. The X-ray source was operated at 30 kV and 30 mA. Diffraction profiles were obtained from the (004) reflection.

3. Epilayer characterization

3.1. GaAs epilayers

The substrate temperatures used for growing the GaAs epilayers ranged from 600 to 875°C; in this range, the carrier concentration measured by the Hall-van der Pauw method increases as the growth temperature is increased. At 650°C, the electron concentration was $\sim 7 \times 10^{15} \text{ cm}^{-3}$, while for samples grown at $\sim 870^\circ\text{C}$, the concentration was $\sim 2 \times 10^{17} \text{ cm}^{-3}$. The samples grown at temperatures under 600°C were *p*-type with relatively low conductivity; in some cases it was not possible to measure them because of the difficulty in obtaining ohmic contacts. Over 650°C, the samples grown were *n*-type with controllable carrier concentration. The detailed conductivity dependence of the epilayers on the growth temperature has been reported in other work [5].

The 10 K photoluminescence (PL) spectra for *p*- and *n*-type GaAs layers are shown in Fig. 1. The PL peak identification is as follows [6,7]:

1. 8183 Å free excitons, (F, X);
2. 8186.7-8187.9 Å excited state bound to neutral donors, $(\text{D}^\circ, \text{X})_{exc}$.
3. 8197 Å $J=1/2$ exciton bound to neutral acceptor, $(\text{A}^\circ, \text{X})_{1/2}$;

the peaks labeled 4 and 5 correspond to conduction band to neutral acceptor at 8301 Å, ($e\text{-A}^\circ$), and neutral donor to neutral acceptor at 8325 Å, ($\text{D}^\circ\text{-A}^\circ$). The existence of the free exciton peak at 8183 Å, labeled 1 in Fig. 1, demonstrates the high quality of the GaAs epilayers. As is usual in the MOCVD process, *p*-type conductivity is related to the carbon acceptor from the metalorganic precursors. Carbon is introduced by TMG pyrolysis, which releases methyl radicals at the GaAs surface. In the traditional MOCVD, the AsH_3 dissociation at the surface produces atomic hydrogen, which diffuses and recombines with methyl radicals to produce the stable and volatile methane (CH_4) [8]. As can be observed in the PL spectra, when the growth temperature is increased, the peaks of the excitonic band disappear and a wide peak corresponding to excited state transitions related to donors and acceptors is observed. Therefore, this result is explained by the increase on the concentration of undesired residual impurities. The donor impurity responsible for the *n*-type conductivity could be related to the silicon metalorganic compounds, the most common impurities of the metalorganic precursors [9].

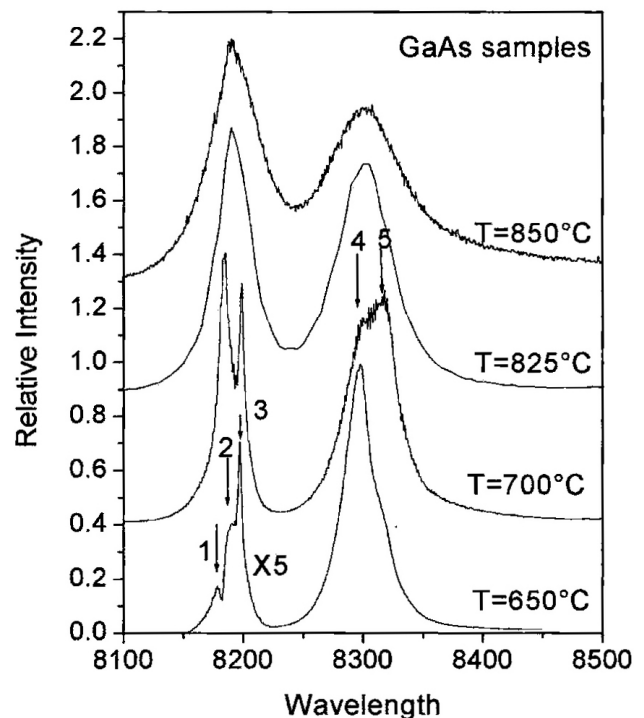


FIGURE 1. PL spectra at 10 K of GaAs samples grown at different substrate temperature conditions.

3.2. $\text{Al}_x\text{Ga}_{1-x}\text{As}$ epilayers

The $\text{Al}_x\text{Ga}_{1-x}\text{As}$ epilayers were grown on a wide interval of substrate temperatures. The $\text{Al}_x\text{Ga}_{1-x}\text{As}$ alloy is much more difficult to grow than GaAs, due to the strong chemical affinity of aluminum to oxygen and carbon [10]. The $\text{Al}_x\text{Ga}_{1-x}\text{As}$ samples growth at temperatures under 800°C highly resistive with a weak luminescence signal. In many cases, the samples presented a hazy surface.

The high resistivity and the weakness of the PL signal on the $\text{Al}_x\text{Ga}_{1-x}\text{As}$ epilayers have been related to the incorporation of oxygen from the residual impurities of the metalorganic precursors [11]. It is widely accepted that oxygen as an impurity introduces deep traps into $\text{Al}_x\text{Ga}_{1-x}\text{As}$ [12]. The three dominating nonradiative deep centers, located at about 0.3, 0.5 and 0.8 eV below the conduction band, critically reduce luminescence efficiency [13]. In addition when the growth temperature is increased, the traps concentration is reduced [14]. Therefore, in order to reduce the oxygen incorporation temperatures over 800°C were chosen for growing the ternary alloy films.

Figure 2 shows a typical PL spectrum of an $\text{Al}_x\text{Ga}_{1-x}\text{As}$ epilayer, corresponding to a sample grown at 850°C ; the arsenic temperature was selected to fix the III/V ratio at 20. In order to easily detect the photoluminescence signal, the amount of metalorganic precursors (TMG and TMAI) supplied to the growth chamber was adjusted for an aluminum mole fraction of $x < 0.3$.

In the spectra in Fig. 2, three peaks are observed: the peaks at 8189 \AA and 8300 \AA come from the GaAs buffer layer. The peak at 7438 \AA is produced by the $\text{Al}_x\text{Ga}_{1-x}\text{As}$

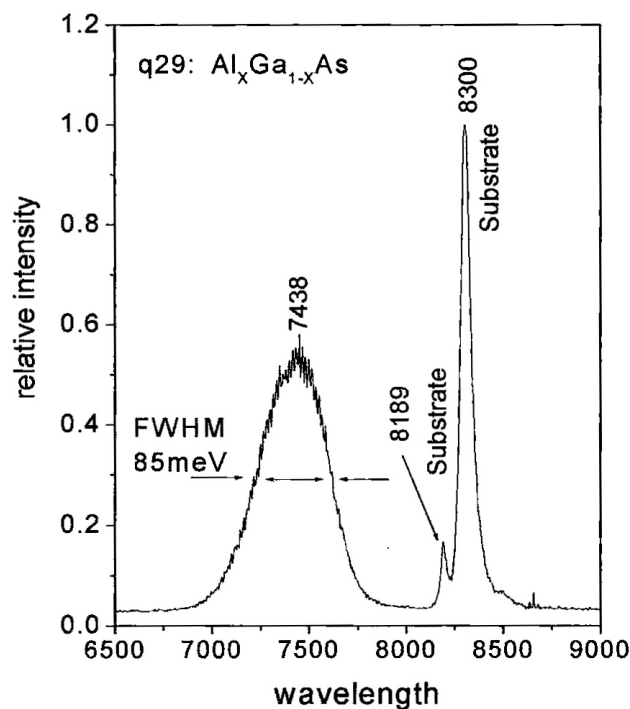


FIGURE 2. Photoluminescence spectra at 10 K on an $\text{Al}_x\text{Ga}_{1-x}\text{As}$ epilayer grown by MOCVD-As at 800°C .

epilayer; this peak involves the excitonic bands and those corresponding to the donor-acceptor transitions. The full wide at half maximum (FWHM) is $\sim 85\text{meV}$, a value that turn out to be large compared with the corresponding value of samples grown by using arsine based-MOCVD or LPE [15]. The large values of FWHM are indicative of a high degree of electrical compensation by incorporation of residual impurities [16]. The weakness of the PL spectra is not directly related to the replacement of arsine by metallic arsenic, but to the chemical purity of the metalorganic precursors and the chemical reactivity of the aluminum to carbon and oxygen. The results reported in the literature, where the excitonic band of $\text{Al}_x\text{Ga}_{1-x}\text{As}$ is clearly seen, correspond to epilayers grown with double or triple distilled TMAI [17]. An equivalent result to the one shown in Fig. 2 is reported in Ref. 18, where the weakness of the PL signal is related to the low chemical purity of the aluminum metalorganic precursor. The problems associated with the metalorganic precursors must be resolved in the future for the fabrication of reliable electronic devices, although the optimization processes for obtaining high quality $\text{Al}_x\text{Ga}_{1-x}\text{As}$ using solid arsenic still remains obscure. Therefore, to reduce the oxygen incorporation and to facilitate the electrical characterization, the $\text{Al}_x\text{Ga}_{1-x}\text{As}$ epilayers were grown in the temperature range of 830 to 875° .

The electrical characterization of the $\text{Al}_x\text{Ga}_{1-x}\text{As}$ samples using the Hall effect was carried out on samples with an aluminum molar concentration of $x = 0.3$; however, any value of molar aluminum concentration could be chosen. The $\text{Al}_x\text{Ga}_{1-x}\text{As}$ epilayers turned out to have an electron concentration of $n \sim 10^{17} \text{ cm}^{-3}$, and a carrier mobility of $\sim 2000 \text{ cm}^2/\text{V*s}$ at room temperature. These results are similar to the values reported in the literature [19].

X-ray diffraction analysis was done on several $\text{Al}_x\text{Ga}_{1-x}\text{As}$ epilayers. X-ray diffraction rocking curves were taken using the $\text{CuK}\lambda$ radiation with a wavelength of $\lambda = 1.540597 \text{ \AA}$, in the vicinity of the (400) plane reflections. With these results, and using Vegard's law, we concluded that in the alternate arsenic based MOCVD system we can also control the molar aluminum concentration from $x = 1$ to $x = 0$. Some results of these measurements are shown in Fig. 3.

4. Growth of QW structures

4.1. Growth procedure

To demonstrate the usefulness of the MOCVD-arsenic based system, several structures containing quantum wells (QW) were grown. A simple QW structure possesses four epitaxial layers arranged in the following order:

- i) an undoped GaAs buffer layer,
- ii) a first $\text{Al}_x\text{Ga}_{1-x}\text{As}$ barrier layer,
- iii) a very thin GaAs layer and

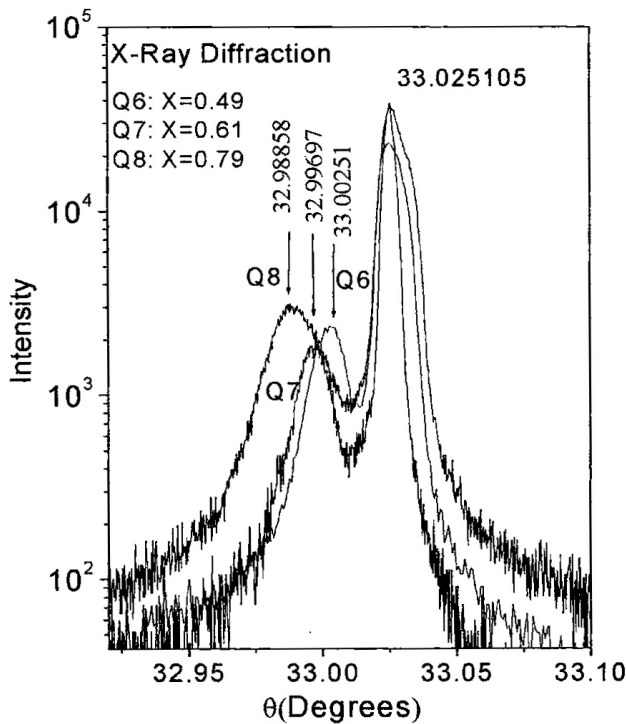


FIGURE 3. X-Ray diffraction measurements on $Al_xGa_{1-x}As$ epilayers with different molar aluminum content.

iv) a second $Al_xGa_{1-x}As$ barrier layer.

The growth of the structures finished with a very thin protective GaAs layer (10-15 nm), to prevent $Al_xGa_{1-x}As$ surface deterioration. In this work, both $Al_xGa_{1-x}As$ barrier layers were grown with the same aluminum molar fraction.

To Obtain the desired characteristics in our structures, we use the following growth procedure: the metallurgical changes were accomplished by opening and closing automatically controlled valves in the TMAI and TMG lines. After the growth of the GaAs buffer layer and the first $Al_xGa_{1-x}As$ barrier (cladding layer), the growth process was interrupted for some time to purge the growth chamber and to produce abrupt interfaces. The interruption times varied from 0 to 15 min. The growth time for growing the intermediate GaAs layer was 25 seconds, enough to growth a quantum well of ~ 10 nm. Figure 5 shows the time diagram

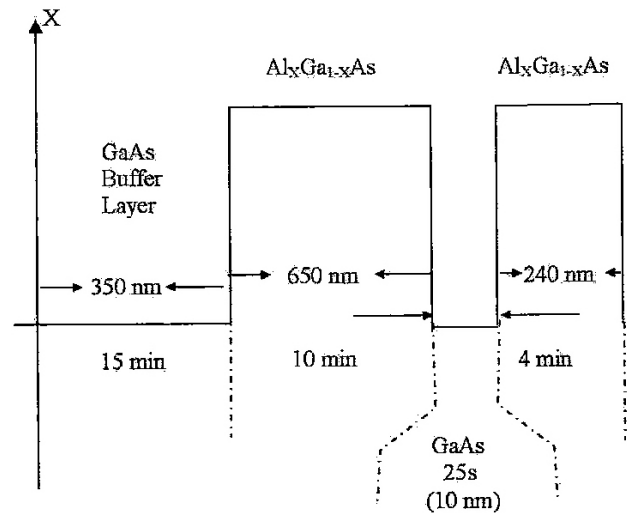


FIGURE 5. Time diagram for growing the QW structures.

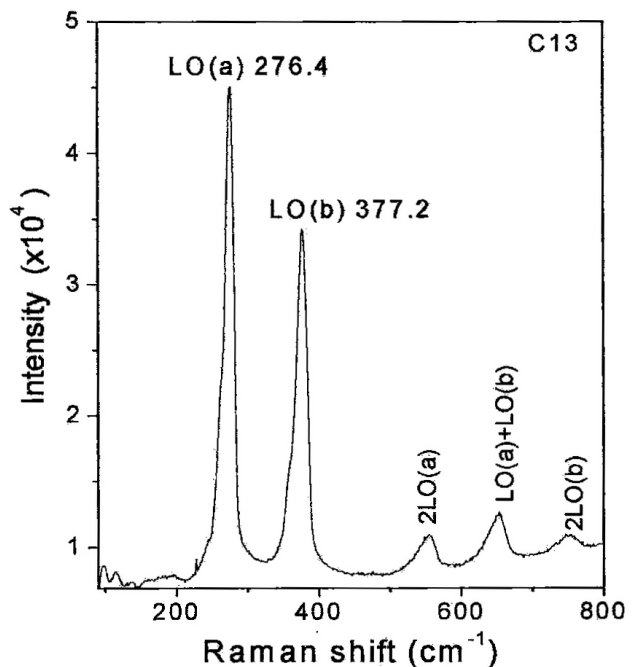


FIGURE 6. Raman spectra of sample C13.

used in growing sample C13 according to the described procedure. The growth rates for the $Al_xGa_{1-x}As$ were $4 \mu m/h$ and $1.4 \mu m/h$ for the GaAs epilayers.

After the growth step for the second $Al_xGa_{1-x}As$ layer, the growth process was stopped and the metalorganic precursor flux was cut off from the growth chamber; there was an interruption time of 6 minutes before the growth of the GaAs protecting layer. To verify the aluminum composition of the cladding layers, the structures were characterized by Raman dispersion. The Raman dispersion results for sample C13 are presented in the Fig. 6.

The composition of the $Al_xGa_{1-x}As$ ternary layers can be estimated using the Raman frequency versus aluminum

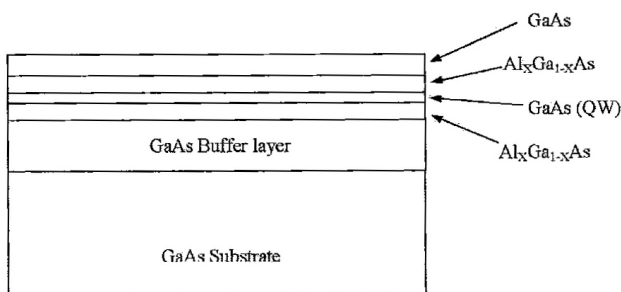


FIGURE 4. Diagram showing a semiconductor structure containing a quantum well.

molar concentration curves in Ref. 20. The aluminum molar concentration (x) can be evaluated from the position of the LO(a) and LO(b) peaks. In the case of sample C13, x was close to 0.3. Additionally, it can be observed that the molar aluminum concentration is the same for both barriers.

4.2. SIMS studies

The chemical composition of the multilayer samples was studied using secondary ion mass spectroscopy (SIMS). The SIMS technique has been successfully used for the evaluation of semiconductor structures with thin layers consisting of only a few monolayers. The analytical parameters for these measurements were Cs^+ as primary ions, and 10 nA as primary current, the beam diameter was $40\mu m$ with an impact energy of 3 KeV, the bombarded area was $150\mu m^2$ and the mass resolution ($M/\Delta M$) was 300.

Figure 7 shows a SIMS composition profile for the sample C14. Figure 7 demonstrates the successful growth of a structure with a single quantum well. The growing process used in grown this structure was similar to sample C13, the GaAs well was grown for 25 seconds, for a thickness of ~ 10 nm. The interrupted time before the growth of the GaAs protecting layer was 2 minutes. The SIMS profile shows a medium thickness of about 46 nm that is much more than we expected, in addition the aluminum concentration curve in the well does not return to the background SIMS level. This behavior can be attributed to the matrix effect [21]. Some of these effects are related to the penetration depth of the ions used for the sample erosion during the SIMS measurement

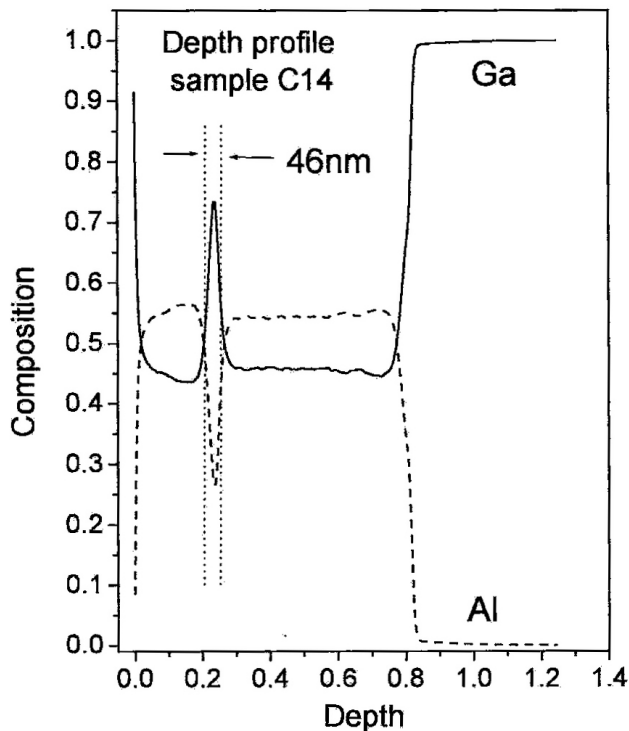


FIGURE 7. Compositional profile by SIMS of a QW structure.

process and the effect of the surface roughness depth resolution, among other factors.

4.3. Surface Roughness

The resulting surface morphology of the multilayer structures was evaluated by AFM measurements. Figure 8 shown the case of sample C14, where the presence of substantial microscopic roughness can be observed, although in the 3D surface image presented, the z scale has been multiplied by 5 in order to show more details. The importance of minimizing surface roughness is for the enhancement of optical and electrical properties. In carrying out this work, several procedures and growth conditions were tried to minimize surface roughness; however, much more work must be done in order to obtain better results when $Al_xGa_{1-x}As$ layers are included [21]. The usual explanation for the high degree of roughness is the very low surface mobility of aluminum during the growth process. Furthermore, as metallic arsenic replaces AsH_3 , the possible change on the surface kinetics processes for arsenic integration must be argued because As_4 is

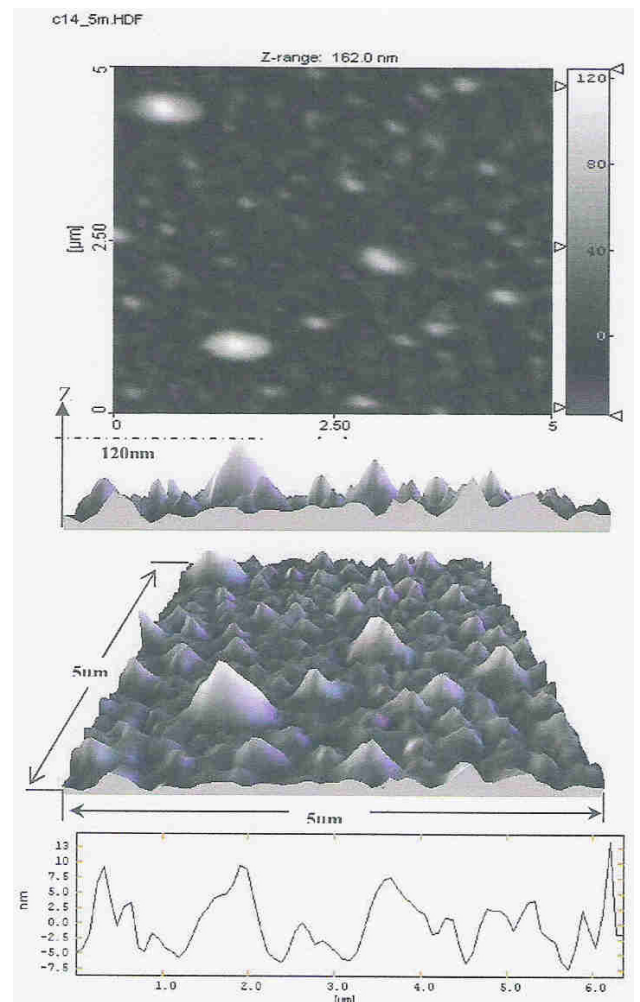


FIGURE 8. AFM microphotograph of the surface morphology. The z scales has been multiplied by 5.

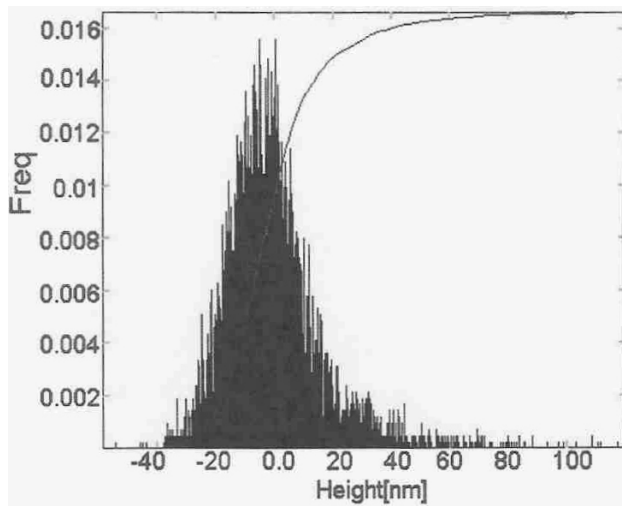


FIGURE 9. The histogram shows the distribution heights on 403 points at the sample surface.

the dominant species. Some other differences can be mentioned between the systems that use AsH_3 and those with solid arsenic, although the detailed processes involved in the surface reactions, diffusion processes and so forth, are not well known yet. The arsenic from the AsH_3 is monoatomic in contrast with As_4 from the case of solid arsenic; the surface processes for aluminum integration also must be modified.

As can be observed, Fig. 9 shows the results of considering the statistical height fluctuations of the surface; the histogram has been compiled from 403 points taken on individual atomic planes perpendicular to the surface. In addition, there are some mountains that have heights greater than 100 nm. This kind of roughness can strongly deteriorate the opti-

cal properties of the quantum well PL emission, due to large thickness distribution as is shown in Fig. 9.

In summary, we have shown that traditional arsine MOCVD can be successfully replaced by the alternative arsenic-based system. Alternative precursor sources have been utilized in order to reduce the risk involved in using AsH_3 ; of these sources, metallic arsenic is the safest. In this work, we have presented the results obtained in the successful growth of $\text{Al}_X\text{Ga}_{1-X}\text{As}/\text{GaAs}/\text{Al}_X\text{Ga}_{1-X}\text{As}$ structures containing quantum wells. An apparent limitation is the amount of surface roughness; however, this result is closely related to the chemical purity of the metalorganic precursors.

5. Conclusions

In conclusion, it was demonstrated that the solid arsenic based MOCVD system permits the growth of $\text{Al}_X\text{Ga}_{1-X}\text{As}/\text{GaAs}/\text{Al}_X\text{Ga}_{1-X}\text{As}$ heterostructures. The main limitation of the alternative MOCVD system is related to the low chemical purity of the metalorganic precursors, especially for aluminum. AFM studies have shown a high degree of roughness on the $\text{Al}_X\text{Ga}_{1-X}\text{As}$ surface. The SIMS studies demonstrate that the system can be useful for the growth of complex structures. However, there must be additional work in order to reduce some problems such as the high compensation of the epitaxial layers, and some problems at the interfaces.

Acknowledgements

This work is supported in part by CONACYT-México under the contract 47104-Y.

1. J.R. Dong *et al.*, *J. Crystal Growth* **289** (2006) 59.
2. R.H. Walling and R.H. Moss, *J. Phys. III.* **2** (1992) 1399.
3. B. Bo *et al.*, *Japan. J. Appl. Phys.* **43**(2004) 3410.
4. R. Peña-Sierra, J.G. Castro-Zavala, and A. Escobosa J, *Crystal Growth* **107**(1991) 337.
5. R. Peña-Sierra, A. Escobosa, and V. M. Sanchez-R. *Appl. Phys. Lett.* **62** (1993) 2359.
6. W.R. Leitch and H.L. Ehlers, *Infrared Phys.* **28** (1988) 433.
7. M. Tirtowidjojo and R. Pollard, *J. Crystal Growth* **93** (1988) 108.
8. L. Pavesi and M. Guzzi, *J. Appl. Phys.* **75** (1994) 4779.
9. G. Parish, S. Keller, S.P. Denbaars, and U.K. Mishra. *J. Electron. Mater.* **29** (2000) 15.
10. G. Wicks, W.I. Wang, C.E. Wood, L.F. Eastman, and L. Rathbun, *J. Appl. Phys* **52** (1981) 5792.
11. A.C. Jones, *Chemical Society Reviews* **26** (1997) 101.
12. M.S. Goorsky *et al.*, *Appl. Phys. Lett.* **58** (1991) 1979.
13. S. Keller, *et al.*, *Japan. J. Appl. Phys.* **44** (2005) pp 7227–7233.
14. J.P. André, M. Boulou, and A. Micrea-Roussel, *J. Crystal Growth* **55** (1981) 192.
15. Y. Shiraki, T. Mishima, and M. Morita, *J. Crystal Growth* **81** (1987) 164.
16. H. Terao and H. Sunakawa, *J. Crys Growth* **68** (1984) 157.
17. G. Xing and Y-Z. Zhen, *J. Microwaves and Optoelectronics* **2** (2002) ISSN 1516-7399.
18. C.R. Abernathy *et al.*, *Appl. Phys. Lett.* **56** (1990) 2654.
19. R.M. Biefeld *et al.*, *J. Cryst. Growth* **163** (1996) 212.
20. S. Perkowitz, “Optical Characterization of Semiconductors” Academic Press Limited, (1994)
21. P. Cusumano *et al.*, *J. Appl. Phys.* **81** (1997) 2445.
22. G.B. Stringfellow, *Organometallic Vapor Phase Epitaxy Theory and Practice*, Academic Press, Inc. Harcourt Brace Jovanovich, Publishers (1989).